

1 **Integrated characterization of SARS-CoV-2 genome,**
2 **microbiome, antibiotic resistance and host response from**
3 **single throat swabs**

4 Bo Lu^{1,2,11}, Yi Yan^{3,4,5,6,11}, Liting Dong^{1,2,11}, Lingling Han^{7,11}, Yawei Liu^{8,11},
5 Junping Yu³, Jianjun Chen^{3,4,5}, Danyang Yi¹, Meiling Zhang¹, Chao Wang⁷,
6 Runkun Wang⁷, Dengpeng Wang^{7*}, Hongping Wei^{3*}, Di Liu^{3,4,5,6,9*} and Chengqi
7 Yi^{1,2,10*}

8 *¹State Key Laboratory of Protein and Plant Gene Research, School of Life Sciences,*
9 *Peking University, Beijing 100871, China*

10 *²Peking-Tsinghua Center for Life Sciences, Peking University, Beijing 100871, China*

11 *³CAS Key Laboratory of Special Pathogens, Wuhan Institute of Virology, Center for*
12 *Biosafety Mega-Science, Chinese Academy of Sciences, Wuhan 430071, China*

13 *⁴National Virus Resource Center, Wuhan Institute of Virology, Chinese Academy of*
14 *Sciences, Wuhan 430071, China*

15 *⁵Computational Virology Group, Center for Bacteria and Viruses Resources and*
16 *Bioinformation, Wuhan Institute of Virology, Chinese Academy of Sciences, Wuhan*
17 *430071, China*

18 *⁶University of Chinese Academy of Sciences, Beijing 101409, China*

19 *⁷GrandOmics Biosciences, Wuhan, Hubei 430000, China*

20 *⁸Department of Gastroenterology, The First Medical Center of PLA General*
21 *Hospital/Chinese PLA Postgraduate Military Medical School, Beijing 100853, China*

22 *⁹First Affiliated Hospital of Xinjiang Medical University, Urumqi 830054, China*

23 *¹⁰Department of Chemical Biology and Synthetic and Functional Biomolecules Center,*
24 *College of Chemistry and Molecular Engineering, Peking University, Beijing 100871, China*

25 *¹¹These authors contributed equally*

26 **Correspondence to: chengqi.yi@pku.edu.cn (C.Y.), liud@wh.iov.cn (D.L.),*
27 *hpwei@wh.iov.cn (H.W.) and wangdp@grandomics.com (D.W.)*

28 **Abstract**

29 The ongoing coronavirus disease 2019 (COVID-19) pandemic, caused by
30 severe acute respiratory syndrome coronavirus 2 (SARS-CoV-2) infection,
31 poses a severe threat to humanity. Rapid and comprehensive analysis of both
32 pathogen and host sequencing data is critical to track infection and inform
33 therapies. In this study, we performed unbiased metatranscriptomic analysis of
34 clinical samples from COVID-19 patients using a newly-developed RNA-seq
35 library construction method (TRACE-seq), which utilizes tagmentation activity
36 of Tn5 on RNA/DNA hybrids. This approach avoids the laborious and time-
37 consuming steps in traditional RNA-seq procedure, and hence is fast, sensitive
38 and convenient. We demonstrated that TRACE-seq allowed integrated
39 characterization of full genome information of SARS-CoV-2, putative pathogens
40 causing coinfection, antibiotic resistance and host response from single throat
41 swabs. We believe that the integrated information will deepen our
42 understanding of pathogenesis and improve diagnostic accuracy for infectious
43 diseases.

44

45 **Keywords:** SARS-CoV-2, COVID-19, metatranscriptomics, coinfection,
46 antibiotic resistance, host response, TRACE-seq, Tn5.

47 **Introduction**

48 Longstanding, emerging, and re-emerging infectious diseases continuously
49 threaten human health across centuries(1). Precise and rapid identification of
50 pathogens from clinical samples is important for both guiding infection
51 treatment strategies and monitoring novel infectious disease outbreaks, e.g.
52 the outbreak of SARS-CoV-2, in the community. While most nucleic acid
53 amplification-based and pathogen specific antibody detection-based molecular
54 techniques only detect a limited number of pathogens and need their prior
55 knowledge, metagenomic or meta-transcriptomic approaches allow for
56 comprehensive and unbiased identification and characterization of microbiome
57 directly from clinical specimens(2).

58

59 Compared to meta-genomic sequencing, meta-transcriptomic sequencing has
60 several distinct advantages: it permits detection of RNA viruses that would not
61 be interpreted in metagenomic data, reveals transcriptionally active organism(s)
62 which are more etiologically important, and indicates host immune response
63 which is essential to distinguish true pathogens from colonizers(3-5). However,
64 the laborious and time-consuming steps in traditional RNA-seq experiments
65 hinder the development of meta-transcriptomic based clinical diagnostics for
66 rapid pathogen identification.

67

68 Very recently, we and others have independently developed a rapid and cost-
69 effective RNA-seq method, based on Tn5 tagmentation activity towards
70 RNA/DNA hybrids(6, 7). Our method, termed “TRACE-seq”, enables rapid one-
71 tube library construction for RNA-seq experiments and shows excellent

72 performance in comparison to traditional RNA-seq methods. We thus
73 envisioned that this convenient and sensitive method could be applied to
74 clinical specimens for unbiased meta-transcriptomic analysis. In this study, we
75 modified the TRACE-seq procedure, shorten the total time and optimized
76 analytical pipeline to meet the needs for clinical meta-transcriptomic diagnosis
77 and analysis. We then applied TRACE-seq to meta-transcriptomic sequencing
78 of single throat swabs specimens from COVID-19 patients and healthy
79 individuals. We found library construction of specimens could be accomplished
80 in ~2h with high quality. Analysis of TRACE-seq meta-transcriptomic data of 13
81 SARS-CoV-2 positive samples and 2 negative samples demonstrated the
82 success of this method to sensitively detect SARS-CoV-2 with high coverage
83 even for samples with relatively high Ct values, or to assemble unknown
84 microbe genome *de novo* (using SARS-CoV-2 as an example). Moreover,
85 TRACE-seq sensitively detected the microbiome and simultaneously allowed
86 for interrogating antibiotic resistance and host responses. Taken together,
87 TRACE-seq enables unbiased pathogen detection and could have broad
88 applications in meta-transcriptomic study and clinical diagnosis.

89

90 **Results**

91 **TRACE-seq enables metatranscriptomic analysis**

92 To perform metatranscriptomic analysis on clinical samples, such as throat
93 swabs in this study, we made several modifications to TRACE-seq. First, to
94 achieve unbiased sequencing of microbiome, we used both random hexamer
95 and oligo d(T)₂₃VN primers for reverse transcription, using approximately 1/10
96 total RNA extracted from a single throat swab as input. Secondly, we reduced

97 the total time of library construction to around 2 hours (Figure 1a), which
98 enables TRACE-seq to be more compatible for clinical use, especially when
99 substantial numbers of specimens require investigation. Third, we developed a
100 tailored analytical pipeline of TRACE-seq to simultaneously identify known and
101 unknown pathogens and at the meanwhile to characterize host transcriptional
102 response in a single metatranscriptomic profiling reaction (Figure 1b). This new
103 pipeline allowed us to obtain rich information from the metatranscriptomic data
104 generated by the modified TRACE-seq.

105

106 **Sensitive detection of SARS-CoV-2 genome**

107 Since the samples were positive or suspected positive throat swabs from
108 COVID-19 patients, we asked whether the untargeted meta-transcriptomic
109 sequencing could yield a full genome sequence of SARS-CoV-2 virus. After
110 removing low quality reads and human reads, the remaining reads were
111 mapped to the SARS-CoV-2 reference genome Wuhan-Hu-1 (accession
112 number: NC_045512). Sequencing covered the reference genome from 171 bp
113 to 29,903 bp (0.57%-100%), with an average sequencing depth from 2.56 \times to
114 44,737 \times (Supplementary table 1). Four samples (B101, A193, B13, C1) with
115 low Ct values showed poor coverage and sequencing depth; the isolated RNA
116 samples from the throat swabs were repeatedly frozen and thawed, probably
117 compromising the integrity of RNA and hence were excluded. The other nine
118 samples were used for subsequent correlation analysis. Among the remaining
119 nine samples, the proportion of obtained reads of SARS-CoV-2, the coverage
120 to the reference genome, the average sequencing depth and the median
121 sequencing depth all showed a negative correlation with the Ct value of the

122 samples (Spearman test, $p < 0.05$) (Figure 2a). In addition, the whole genome
123 sequence could be acquired from mapping-based approach when the Ct value
124 is as high as 32 ($n=4$, 44.44% of samples), with the average sequencing depth
125 of 131 \times . Even in samples with Ct values up to 35 ($n=7$, 77.78% of samples),
126 more than 94% of genome can be covered by TRACE-seq (Figure 2b,
127 Supplementary table 1, Supplementary figure 1).

128

129 **Reconstruction of full-length genome of SARS-CoV-2**

130 Of the 452,865 contigs (average 34,836, from 18,160 to 53,415) assembled *de-*
131 *novo* from non-human reads, 3,500 contigs (average 269, from 0 to 2,976) were
132 determined to be SARS-CoV-2 genome fragments. There were no SARS-CoV-
133 2 contigs in sample C31, B101 and B13. Most of contigs ($n=3,461$, 98.89%)
134 were less than 1,000 bp (Figure 2c). To determine the accuracy of this method
135 in acquisition of pathogen genome, all SARS-CoV-2 contigs were searched
136 against genomes of each sample. In contigs with matched length over 1,000
137 bp, most contigs (22/39, 56.41%) were completely consistent with their
138 corresponding genome (Figure 2d), while the other contigs had error bases
139 from 1 to 7. In samples C14 and C13 with excellent coverage and depth, almost
140 full-length genome (29,793 bp and 29,825 bp) were obtained just from *de-novo*
141 assembly. Thus, TRACE-seq could enable the *de-novo* assembly of the
142 complete genome of unknown pathogens and be readily utilized to identify
143 emerging pathogens in patients with unknown etiology of infection and
144 efficiently complement routine diagnostics.

145

146 **Unbiased identification of putative pathogens in addition to SARS-CoV-2**

147 It is widely reported that coinfection (multi-species infection) contributes to
148 enhanced morbidity and mortality, especially in elderly and immunosuppressed
149 influenza patients(8, 9). Thus, we were curious to see if our metatranscriptomic
150 sequencing approach could capture other pathogens in addition to SARS-CoV-
151 2. Indeed, alignment of TRACE-seq data to microbe reference databases
152 identified many bacteria, fungi and viruses in both patient and healthy samples
153 (Figure 3a). To assess whether COVID-19 patients and healthy individuals have
154 different microbe community in their throat, principal coordinates analysis
155 (PCoA) was conducted using relative abundance of the microbiome. We
156 observed that COVID-19 patients harbored a throat microbiome that is quite
157 different from healthy individuals (Figure 3b). In addition, sample C31 differed
158 significantly from other SARS-CoV-2 positive samples. Further investigation of
159 the relative abundance of probable respiratory pathogens revealed that patient
160 C31 contained the most abundant *Klebsiella pneumoniae* and Human
161 gammaherpesvirus 4, compared to other samples (Figure 3c), which might be
162 a cause of the separation between sample C31 and the rest of the SARS-CoV-
163 2 positive samples.

164
165 Among the probable respiratory pathogens listed in Figure 3c,
166 *Stenotrophomonas maltophilia*, *Haemophilus parainfluenzae*, *Staphylococcus*
167 *aureus*, *Streptococcus pneumoniae*, *Haemophilus influenzae* and
168 *Acinetobacter baumannii* are common commensal organism of the normal
169 oropharynx, however, they can also become opportunistic pathogens and
170 cause infectious disease, such as endocarditis, bacteremia and pneumonia(10-
171 13). *Klebsiella pneumoniae*, *Stenotrophomonas maltophilia*, *Pseudomonas*

172 *aeruginosa*, *Neisseria meningitidis* and *Legionella pneumophila* cause disease
173 infrequently in normal hosts but can be a major cause of infection in patients
174 with underlying or immunocompromising conditions(14-18). *Mycoplasma*
175 *pneumoniae* is a type of “atypical” bacteria that commonly causes mild
176 infections of the respiratory system(19). As for identified fungi, *Candida*
177 *dubliniensis* and *Candida albicans* are both opportunistic yeast and can be
178 detected in the gastrointestinal tract in healthy adults; they were also known to
179 cause respiratory diseases (20-22). Human respirovirus 1, also known as
180 Human parainfluenza virus 1, is the most common cause of croup and also
181 associated with pneumonia. Human gammaherpesvirus 4 is one of the most
182 common viruses in human; it is best known as the cause of infectious
183 mononucleosis (23, 24), and is also constantly detected in lungs of patients with
184 idiopathic pulmonary fibrosis (25). In our results, a relatively high abundance of
185 *Haemophilus parainfluenzae*, *Streptococcus pneumoniae*, *Acinetobacter*
186 *baumannii*, *Pseudomonas aeruginosa* and *Neisseria meningitidis* were
187 identified in several SARS-CoV-2 positive samples compared with negative
188 samples, which indicated potential coinfection. Nevertheless, these data by
189 itself could not prove that COVID-19 patients were coinfected by these
190 identified microorganism; these data have to be carefully interpreted in the
191 clinical context.

192

193 **Profiles of antibiotic resistance genes**

194 Antimicrobial resistance has become a global issue. Pathogens with antibiotic
195 resistance are increasing and many pathogens are becoming multidrug-
196 resistant (26, 27). To characterize antibiotic resistance gene expression profiles,

197 we aligned metatranscriptomic reads against the Comprehensive Antibiotic
198 Resistance Database (CARD) (28). On average, around 84 antibiotic
199 resistance genes were identified in SARS-CoV-2 positive samples, while only
200 around 23 genes were identified in negative samples. According to the CARD,
201 the identified antibiotic resistance genes confer resistance to 23 classes of
202 antibiotics. Almost all resistance gene classes were more abundant in COVID-
203 19 patients compared to healthy individuals. Genes conferring resistance to
204 beta-lactam, aminoglycoside, tetracycline, phenicol, rifamycin, fluoroquinolone
205 and macrolide were the most abundant (Figure 3d). Overall, the distinct
206 microbiome, emergence of potential coinfection, and the elevated abundance
207 of antibiotic resistance genes provide new data for establishing clinical
208 therapeutic scheme during the treatment for COVID-19 patients.

209

210 **Characterization of host response to SARS-CoV-2**

211 Distinguishing infection from colonization remains challenging. Because host
212 transcriptional profiling has emerged as a promising diagnostic tool for
213 infectious diseases (29, 30), we next tested whether the host response to
214 SARS-CoV-2 could be simultaneously characterized by TRACE-seq mediated
215 metatranscriptomic analysis from throat swabs. As shown in Figure 3a, a
216 substantial percentage of the reads are derived from human, and an average
217 of 14,766 human genes with FPKM > 1 were detected per sample (Figure 4a,
218 Figure S2a and b). Based on the gene expression profiles, the relationships
219 between samples were inspected using a multidimensional scaling (MDS) plot
220 (Figure 4b). As expected, SARS-CoV-2 positive samples were clearly
221 separated from negative samples. In addition, sample C31 differed significantly

222 in host gene expression from other SARS-CoV-2 positive samples, which might
223 be caused by the relatively high abundance of Klebsiella pneumoniae and
224 Human gammaherpesvirus 4 identified in sample C31. To characterize the
225 common host response to SARS-CoV-2, we excluded sample C31 when
226 performing differential gene expression analysis between SARS-CoV-2 positive
227 and negative samples. We identified 153 differentially expressed genes, 149 of
228 which were up-regulated (Figure 4c, Figure S2c). Gene Ontology enrichment
229 analysis identified the top up-regulated biological processes to be immune
230 response, defense response, viral process and response to cytokine (Figure
231 4d). Further investigation revealed that a subset of up-regulated genes involve
232 in IL1B-associated inflammatory response (IL1B, IL8, IL36A, CXCR2, FOS,
233 ANXA1, CASP4, KRT16, S100A8, S100A9). Moreover, another subset of up-
234 regulated genes (ISG15, EGR1, IFI27, IFIT2, IFIT3, IFITM1, IFITM2, IFITM3,
235 HLA-B, HLA-C) were enriched in type I interferon signaling pathway (Figure 4e).
236 These results were highly consistent with previously reported host response to
237 SARS-CoV-2 (31-33). Overall, metatranscriptomic data via TRACE-seq of
238 throat swab samples demonstrates reliable performance in characterization of
239 host transcriptional response to the infection of SARS-CoV-2.

240

241 **Discussion**

242 Although next generation sequencing holds a great potential to directly detect
243 known and unknown pathogens including viruses, bacteria, fungi and parasites
244 in a single application, the laborious and time-consuming steps in traditional
245 RNA library construction procedure hinders its clinical application. As a rapid
246 and convenient one-tube RNA-seq library construction method, TRACE-seq

247 significantly lower the barrier for extensive application of unbiased RNA-seq in
248 clinical diagnosis. In addition, multiplexing libraries by utilizing Tn5 transposase
249 containing barcoded adaptors could enable sample investigation in a high-
250 throughput manner, particularly when comprehensive surveillance for emerging
251 pathogens is needed during a sudden disease outbreak.

252

253 It is very challenging to discriminate pathogens from background commensal
254 microbiota, since substantive bacteria or fungi can colonize multiple body sites
255 of healthy individuals. The microbe present at a relatively higher abundance in
256 patients compared to healthy individuals are often considered as a pathogen,
257 yet the abundance thresholds indicating infection is difficult to define based
258 solely on microbiome information. On the other hand, host transcriptional
259 profiling has been reported to distinguish infectious and noninfectious diseases
260 (30) and to further discriminate between viral and bacterial infections (29). A
261 previous study integrates host response and unbiased microbe detection for
262 lower respiratory tract infection diagnosis in critically ill adults, using both RNA-
263 seq and DNA-seq but yet lacking antibiotic resistance analysis (3). Another
264 study characterized microbial gene expression profiles (including antibiotic
265 resistance genes) using nasal and throat swab samples, and host response
266 using blood samples during influenza infection (34). To our knowledge, this is
267 the first study integrating unbiased pathogens detection, antibiotic resistance
268 and host response in a single approach with throat swabs from COVID-19
269 patients. In our results, SARS-CoV-2 positive and negative samples differed
270 significantly in both microbiome composition and host response. Among SARS-
271 CoV-2 positive samples, sample C31 harbored a throat microbiome and host

272 response notably distinct from others, indicating sufficiently different pathogens
273 present in patient C31 compared to other samples. Moreover, TRACE-seq hold
274 the potential to construct a network of microbiome composition, antibiotic
275 resistance and host response for characterizing the complex host-microbiome
276 interactions. Ideally, TRACE-seq data can be utilized to develop a model
277 combining pathogens metric, antibiotic resistance and host transcriptional
278 classifier for infectious diseases diagnosis. We believe that the integrated
279 information acquired from a TRACE-seq library will deepen our understanding
280 of pathogenesis, improve diagnostic accuracy and more precisely inform
281 optimal antimicrobial treatment for infectious diseases caused by not only
282 SARS-CoV-2 but also other pathogens and eventually facilitate the utility of
283 metatranscriptomic profiling as a routine diagnostic method.

284

285 **Materials and methods**

286 **Ethics statement**

287 The study and use of all samples were approved by the Ethics Committee of
288 Wuhan Institute of Virology (No. WIVH17202001).

289

290 **Sample collection and nucleotide extraction**

291 Respiratory specimens (swabs) collected from patients admitted to various
292 Wuhan health care facilities were immediately placed into sterile tubes
293 containing 3 ml of viral transport media (VTM). The swabs were deactivated by
294 heating at 56°C for 30 minutes in a biosafety level 2 (BSL 2) laboratory at the
295 Wuhan Institute of Virology in Zhengdian Park with personal protection
296 equipment for biosafety level 3 (BSL 3) laboratory. Total nucleic acids were

297 extracted using QIAamp 96 virus Qiacube HT kit on QIAxtractor Automated
298 extraction (Qiagen, US) following the manufacturer's instructions.

299

300 **TRACE-seq library preparation and sequencing**

301 TRACE-seq libraries were constructed using TruePrep® RNA Library Prep Kit
302 for Illumina (Vazyme, TR502-01) according to the manufacturer's instructions
303 with several modifications. 1/10 volume of total nucleic acids extracted from
304 each swab was used for each library. After 18 PCR cycles, the library was
305 purified using 0.8X Agencourt AMPure XP beads (Beckman Coulter) and eluted
306 in 20 μ l nuclease-free water. The concentration of resulting libraries was
307 determined by Qubit 3.0 fluorometer with the Qubit dsDNA HS Assay kit
308 (Invitrogen) and the size distribution of libraries was assessed by Agilent 2100
309 Bioanalyzer. Finally, libraries were sequenced on the Illumina Hiseq X10
310 platform which generated 2 x 150 bp of paired-end raw reads.

311

312 **Data preprocessing**

313 Raw reads from sequencing were firstly subjected to Trim Galore (v0.6.4_dev)
314 (http://www.bioinformatics.babraham.ac.uk/projects/trim_galore/) for quality
315 control and adaptor trimming. The minimal threshold of quality was 20, and the
316 minimal length of reads to remain was set as 20 nt.

317

318 **Host transcriptional profiling analysis**

319 Filtered reads were mapped to human genome (hg19) and transcriptome using
320 STAR (v2.7.1a) (35). The FPKM value for annotated genes was calculated by
321 cuffnorm (v2.2.1) (36), and genes with FPKM > 1 were considered to be

322 expressed. Multidimensional scaling and differential gene expression analysis
323 were conducted using EdgeR (v3.28.1) (37) with gene count data generated by
324 HTSeq (v0.11.2) (38). Gene Ontology Enrichment Analysis for biological
325 processes was performed by DAVID (v6.8) (39) with all significantly up-
326 regulated genes as input. Due to the redundancy of enriched GO terms, GO
327 terms and their p values were further summarized using REViGO (40). The top
328 10 enriched representative GO terms were plotted.

329

330 **Discrimination and de-novo assembly of SARS-CoV-2**

331 After removal of human reads, the remaining data were aligned to the reference
332 genome of Wuhan-Hu-1 (GenBank accession number: NC_045512) using
333 Bowtie2 (v2.2.9) (41) for SARS-CoV-2 identification. The coverage and
334 sequencing depth of SARS-CoV-2 genome were calculated by Samtools (v1.9)
335 (42). On the other hand, to verify the method could screen for aetiological agents
336 and obtain pathogen genome, all non-human reads were processed for de-
337 novo assembly using MEGAHIT (v1.2.9) with default parameters (43), and then
338 all contigs were searched against NCBI nt database using blastn for
339 classification(44). As for accuracy of assembly sequences, contigs determined
340 to come from SARS-CoV-2 were performed blastn (with the parameter “-outfmt
341 3”) to display the differences with corresponding genome.

342

343 **Microbiome analysis**

344 After removing human reads, the remaining reads were subjected to microbial
345 taxonomic classification using Kraken2 (v2.0.8-beta) (45) with a custom
346 database. To build the custom database, standard RefSeq complete bacterial

347 genomes were downloaded through “kraken2-build --download-library bacteria”
348 and complete genomes of human viruses and genome assemblies of fungi
349 were downloaded from NCBI’s RefSeq and added to the custom database’s
350 genomic library using the “--add-to-library” switch. Principal coordinate analysis
351 (PCoA) of relative abundances of microbial taxa at the genus level was done
352 using cmdscale command in R. Distances between samples were calculated
353 using Morisita-horn dissimilarity index by vegdist command from vegan
354 package version 2.5-6 (<https://CRAN.R-project.org/package=vegan>). The
355 antibiotic resistance genes were annotated by aligning the filtered
356 metatranscriptomic reads to the Comprehensive Antibiotic Resistance
357 Database (CARD). Antibiotic resistance genes with more than 10 completely
358 matching reads were considered. The relative expression of antibiotic
359 resistance genes were determined as RPM (reads per million non-host reads).
360 All corresponding graphs were plotted using R scripts by RStudio (v1.2.5033)
361 (<https://rstudio.com/>).

362

363 **Acknowledgments**

364 The authors would like to thank Vazyme Biotech in Nanjing, China, for assisting
365 in library procedure optimization and providing library preparation kits. In
366 addition, the authors would like to thank National Center for Protein Sciences
367 at Peking University in Beijing, China, for assistance with experiments. Part of
368 the analysis was performed on the High Performance Computing Platform of
369 the Center for Life Science (Peking University). This work was supported by
370 International Innovation Resource Cooperation Project, Beijing Municipal
371 Science and Technology Commission (No. to C.Y.), National Natural Science

372 Foundation of China (nos. 31861143026, 91740112 and 21825701 to C.Y.) and
373 Epidemic Prevention and Control Special Project, Peking University.

374

375 **Conflict of interests**

376 The authors have filed patents related to TRACE-seq applications.

377

378 **Contributions**

379 C.Q.Y. and D.L. conceived the project; C.Q.Y., D.L., H.P.W., and D.P.W.
380 supervised the project; B.L., Y.Y., and L.T.D. designed the experiments together
381 and wrote the manuscript; L.L.H. performed experiments with the help of C.W.
382 and R.W.; B.L. and Y.Y. performed the bioinformatics analysis; J.P.Y. collected
383 the clinical samples; J.J.C., D.Y.Y., M.L.Z., and Y.W.L. participated in discussion.

384

385 **References**

- 386 1. Lozano R, Naghavi M, Foreman K, Lim S, Shibuya K, Aboyans V, et al. Global and regional
387 mortality from 235 causes of death for 20 age groups in 1990 and 2010: a systematic analysis for
388 the Global Burden of Disease Study 2010. Lancet. 2012;380(9859):2095-128.
- 389 2. Chiu CY, Miller SA. Clinical metagenomics. Nature reviews Genetics. 2019;20(6):341-55.
- 390 3. Langelier C, Kalantar KL, Moazed F, Wilson MR, Crawford ED, Deiss T, et al. Integrating host
391 response and unbiased microbe detection for lower respiratory tract infection diagnosis in critically
392 ill adults. Proceedings of the National Academy of Sciences of the United States of America.
393 2018;115(52):E12353-E62.
- 394 4. Langelier C, Zinter MS, Kalantar K, Yanik GA, Christenson S, O'Donovan B, et al. Metagenomic
395 Sequencing Detects Respiratory Pathogens in Hematopoietic Cellular Transplant Patients. Am J
396 Respir Crit Care Med. 2018;197(4):524-8.
- 397 5. Gliddon HD, Herberg JA, Levin M, Kaforou M. Genome-wide host RNA signatures of
398 infectious diseases: discovery and clinical translation. Immunology. 2018;153(2):171-8.
- 399 6. Lu B, Dong L, Yi D, Zhang M, Zhu C, Li X, et al. Transposase-assisted fragmentation of
400 RNA/DNA hybrid duplexes. Elife. 2020;9.
- 401 7. Di L, Fu Y, Sun Y, Li J, Liu L, Yao J, et al. RNA sequencing by direct fragmentation of RNA/DNA
402 hybrids. Proceedings of the National Academy of Sciences of the United States of America.
403 2020;117(6):2886-93.

404 8. Fischer N, Indenbirken D, Meyer T, Lutgehetmann M, Lellek H, Spohn M, et al. Evaluation of
405 Unbiased Next-Generation Sequencing of RNA (RNA-seq) as a Diagnostic Method in Influenza
406 Virus-Positive Respiratory Samples. *J Clin Microbiol.* 2015;53(7):2238-50.

407 9. Chertow DS, Memoli MJ. Bacterial coinfection in influenza: a grand rounds review. *JAMA.*
408 2013;309(3):275-82.

409 10. Man WH, de Steenhuijsen Piters WA, Bogaert D. The microbiota of the respiratory tract:
410 gatekeeper to respiratory health. *Nat Rev Microbiol.* 2017;15(5):259-70.

411 11. Mitchell JL, Hill SL. Immune response to *Haemophilus parainfluenzae* in patients with chronic
412 obstructive lung disease. *Clin Diagn Lab Immunol.* 2000;7(1):25-30.

413 12. Smeltzer MS. *Staphylococcus aureus* Pathogenesis: The Importance of Reduced Cytotoxicity.
414 *Trends Microbiol.* 2016;24(9):681-2.

415 13. Howard A, O'Donoghue M, Feeney A, Sleator RD. *Acinetobacter baumannii*: an emerging
416 opportunistic pathogen. *Virulence.* 2012;3(3):243-50.

417 14. Paczosa MK, Mecsas J. *Klebsiella pneumoniae*: Going on the Offense with a Strong Defense.
418 *Microbiol Mol Biol Rev.* 2016;80(3):629-61.

419 15. Brooke JS. *Stenotrophomonas maltophilia*: an emerging global opportunistic pathogen. *Clin
420 Microbiol Rev.* 2012;25(1):2-41.

421 16. Sadikot RT, Blackwell TS, Christman JW, Prince AS. Pathogen-host interactions in
422 *Pseudomonas aeruginosa* pneumonia. *Am J Respir Crit Care Med.* 2005;171(11):1209-23.

423 17. Overturf GD. Indications for the immunological evaluation of patients with meningitis. *Clin
424 Infect Dis.* 2003;36(2):189-94.

425 18. Kumpers P, Tiede A, Kirschner P, Girke J, Ganser A, Peest D. Legionnaires' disease in
426 immunocompromised patients: a case report of *Legionella longbeachae* pneumonia and review
427 of the literature. *J Med Microbiol.* 2008;57(Pt 3):384-7.

428 19. Kashyap S, Sarkar M. Mycoplasma pneumonia: Clinical features and management. *Lung India.*
429 2010;27(2):75-85.

430 20. AbdulWahab A, Salah H, Chandra P, Taj-Aldeen SJ. Persistence of *Candida dubliniensis* and
431 lung function in patients with cystic fibrosis. *BMC Res Notes.* 2017;10(1):326.

432 21. Shweihat Y, Perry J, 3rd, Shah D. Isolated *Candida* infection of the lung. *Respir Med Case Rep.*
433 2015;16:18-9.

434 22. Wahab AA, Taj-Aldeen SJ, Kolecka A, ElGindi M, Finkel JS, Boekhout T. High prevalence of
435 *Candida dubliniensis* in lower respiratory tract secretions from cystic fibrosis patients may be
436 related to increased adherence properties. *Int J Infect Dis.* 2014;24:14-9.

437 23. Stanfield BA, Luftig MA. Recent advances in understanding Epstein-Barr virus. *F1000Res.*
438 2017;6:386.

439 24. Dunmire SK, Hogquist KA, Balfour HH. Infectious Mononucleosis. *Curr Top Microbiol
440 Immunol.* 2015;390(Pt 1):211-40.

441 25. Tang YW, Johnson JE, Browning PJ, Cruz-Gervis RA, Davis A, Graham BS, et al. Herpesvirus
442 DNA is consistently detected in lungs of patients with idiopathic pulmonary fibrosis. *J Clin
443 Microbiol.* 2003;41(6):2633-40.

444 26. Boolchandani M, D'Souza AW, Dantas G. Sequencing-based methods and resources to study
445 antimicrobial resistance. *Nature reviews Genetics.* 2019;20(6):356-70.

446 27. Tillotson GS, Zinner SH. Burden of antimicrobial resistance in an era of decreasing
447 susceptibility. *Expert Rev Anti Infect Ther.* 2017;15(7):663-76.

448 28. McArthur AG, Waglechner N, Nizam F, Yan A, Azad MA, Baylay AJ, et al. The comprehensive
449 antibiotic resistance database. *Antimicrob Agents Chemother*. 2013;57(7):3348-57.

450 29. Suarez NM, Bunsow E, Falsey AR, Walsh EE, Mejias A, Ramilo O. Superiority of transcriptional
451 profiling over procalcitonin for distinguishing bacterial from viral lower respiratory tract infections
452 in hospitalized adults. *J Infect Dis*. 2015;212(2):213-22.

453 30. Tsalik EL, Henao R, Nichols M, Burke T, Ko ER, McClain MT, et al. Host gene expression
454 classifiers diagnose acute respiratory illness etiology. *Sci Transl Med*. 2016;8(322):322ra11.

455 31. Lee JS, Park S, Jeong HW, Ahn JY, Choi SJ, Lee H, et al. Immunophenotyping of COVID-19
456 and influenza highlights the role of type I interferons in development of severe COVID-19. *Sci
457 Immunol*. 2020;5(49).

458 32. Zhou Z, Ren L, Zhang L, Zhong J, Xiao Y, Jia Z, et al. Heightened Innate Immune Responses
459 in the Respiratory Tract of COVID-19 Patients. *Cell Host Microbe*. 2020;27(6):883-90 e2.

460 33. Ong EZ, Chan YFZ, Leong WY, Lee NMY, Kalimuddin S, Haja Mohideen SM, et al. A Dynamic
461 Immune Response Shapes COVID-19 Progression. *Cell Host Microbe*. 2020;27(6):879-82 e2.

462 34. Zhang L, Forst CV, Gordon A, Gussin G, Geber AB, Fernandez PJ, et al. Characterization of
463 antibiotic resistance and host-microbiome interactions in the human upper respiratory tract
464 during influenza infection. *Microbiome*. 2020;8(1):39.

465 35. Dobin A, Davis CA, Schlesinger F, Drenkow J, Zaleski C, Jha S, et al. STAR: ultrafast universal
466 RNA-seq aligner. *Bioinformatics*. 2013;29(1):15-21.

467 36. Trapnell C, Williams BA, Pertea G, Mortazavi A, Kwan G, van Baren MJ, et al. Transcript
468 assembly and quantification by RNA-Seq reveals unannotated transcripts and isoform switching
469 during cell differentiation. *Nat Biotechnol*. 2010;28(5):511-5.

470 37. Robinson MD, McCarthy DJ, Smyth GK. edgeR: a Bioconductor package for differential
471 expression analysis of digital gene expression data. *Bioinformatics*. 2010;26(1):139-40.

472 38. Anders S, Pyl PT, Huber W. HTSeq--a Python framework to work with high-throughput
473 sequencing data. *Bioinformatics*. 2015;31(2):166-9.

474 39. Huang da W, Sherman BT, Lempicki RA. Systematic and integrative analysis of large gene lists
475 using DAVID bioinformatics resources. *Nat Protoc*. 2009;4(1):44-57.

476 40. Supek F, Bosnjak M, Skunca N, Smuc T. REVIGO summarizes and visualizes long lists of gene
477 ontology terms. *PLoS One*. 2011;6(7):e21800.

478 41. Langmead B, Salzberg SL. Fast gapped-read alignment with Bowtie 2. *Nature methods*.
479 2012;9(4):357-9.

480 42. Li H, Handsaker B, Wysoker A, Fennell T, Ruan J, Homer N, et al. The Sequence
481 Alignment/Map format and SAMtools. *Bioinformatics*. 2009;25(16):2078-9.

482 43. Li D, Liu CM, Luo R, Sadakane K, Lam TW. MEGAHIT: an ultra-fast single-node solution for
483 large and complex metagenomics assembly via succinct de Bruijn graph. *Bioinformatics*.
484 2015;31(10):1674-6.

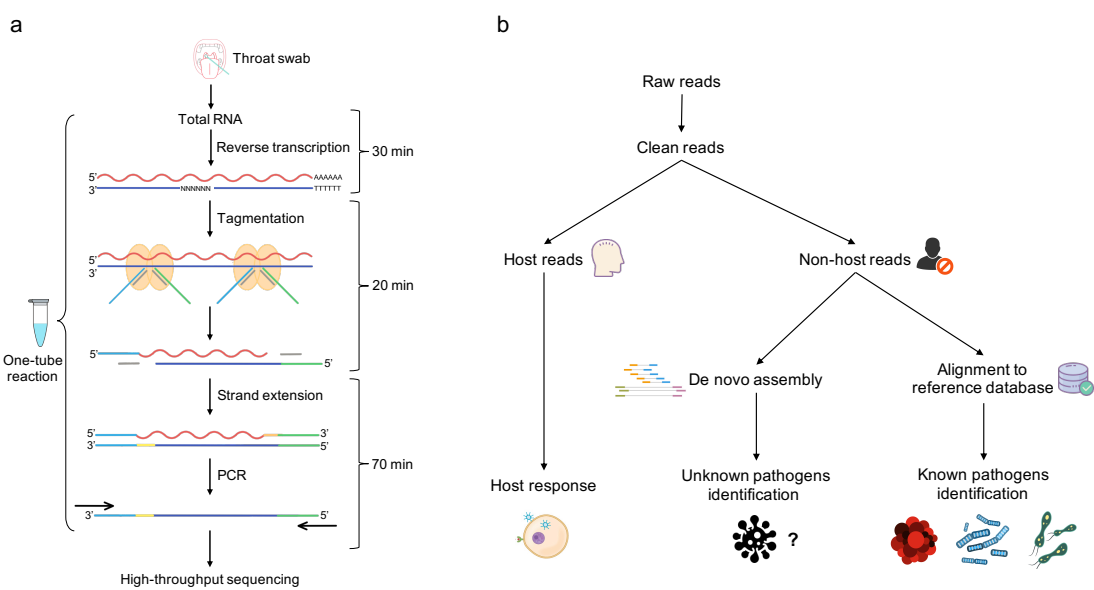
485 44. Camacho C, Coulouris G, Avagyan V, Ma N, Papadopoulos J, Bealer K, et al. BLAST+:
486 architecture and applications. *BMC Bioinformatics*. 2009;10:421.

487 45. Wood DE, Lu J, Langmead B. Improved metagenomic analysis with Kraken 2. *Genome Biol*.
488 2019;20(1):257.

489

490

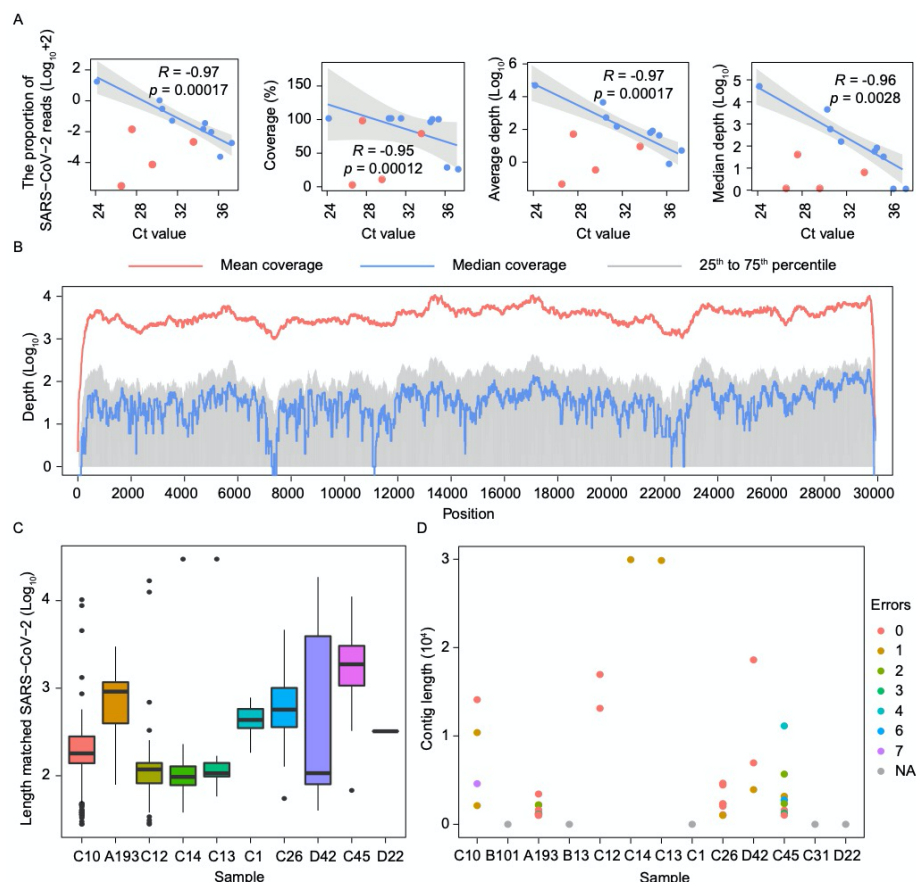
491



492

493 **Figure 1.** Workflow of TRACE-seq enabled metatranscriptomic sequencing for
494 clinical diagnosis. **a.** A wet lab protocol of TRACE-seq starting with total RNA
495 extracted from throat swabs of COVID-19 patients. **b.** A dry lab pipeline
496 including known and unknown pathogens identification and host response
497 characterization.

498

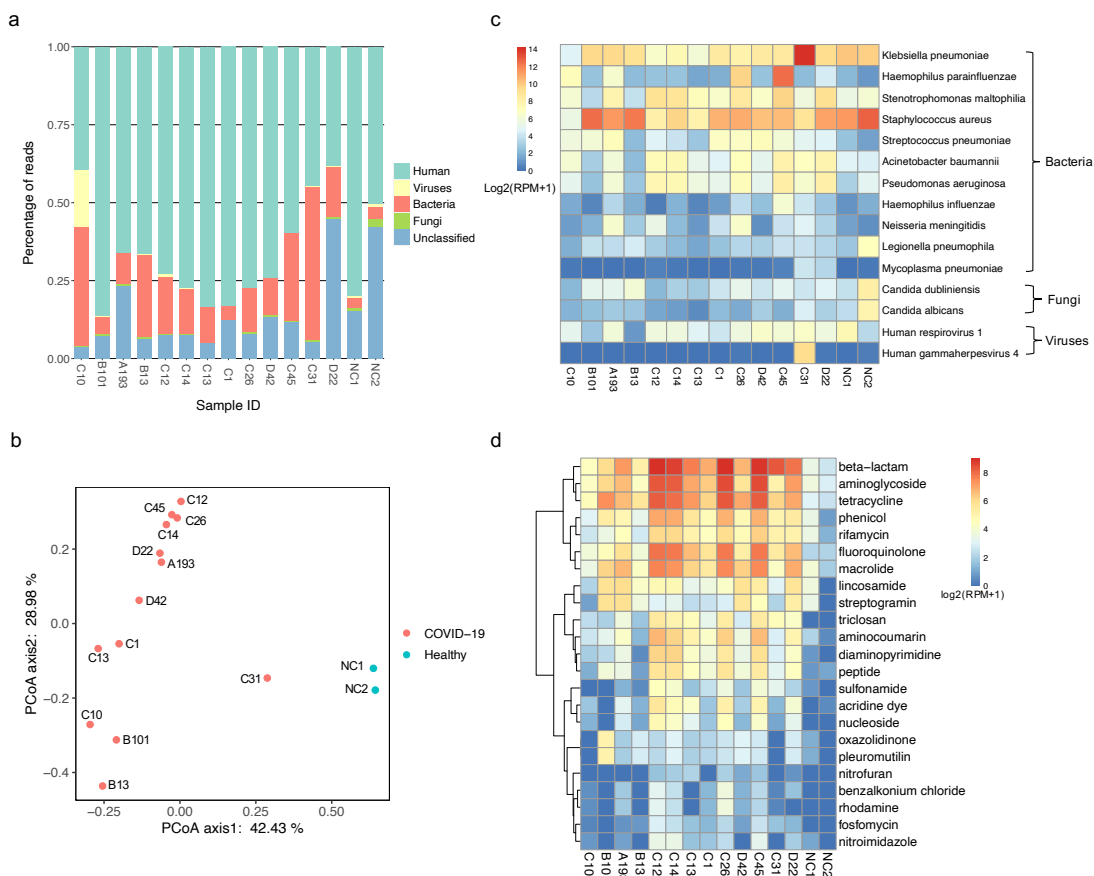


499

500 **Figure 2.** Genome coverage of SARS-CoV-2. **a.** Correlation between SARS-
501 CoV-2 sequencing reads and Ct value in 13 positive samples. From the left
502 to the right: the correlation of the ratio of SARS-CoV-2 reads, the coverage
503 of SARS-CoV-2 genome, the average sequencing depth, the median
504 sequencing depth and the Ct value of each sample are shown in order. The
505 red dots represent samples with abnormal sequencing results, and linear
506 regression indicates the relationship between the sequencing data and the
507 Ct value of samples with normal sequencing results (blue dots). **b.** Genome
508 coverage of sequenced samples across the SARS-CoV-2 genome. The x
509 axis represents the virus genome position, y axis represents the \log_{10} depth
510 of each site. Lines in red represent the mean sequencing depth, lines in blue
511 represent the median sequencing depth, and areas in grey represent 25th to

512 75th percentile of sequencing depth. **c.** Length distribution of contigs matched
513 SARS-CoV-2. The x axis represents each sample, and the y axis represents
514 \log_{10} lengths of contigs matched SARS-CoV-2. **d.** De novo assembly results
515 of SARS-CoV-2. The graph shows contigs only when the length of matched
516 to the SARS-COV-2 genome over 1,000 bp. The y axis represents length of
517 contigs of each sample (the x axis). Different colors represent the number of
518 error bases (shown in legends) in each contig relative to previously known
519 genome sequences.

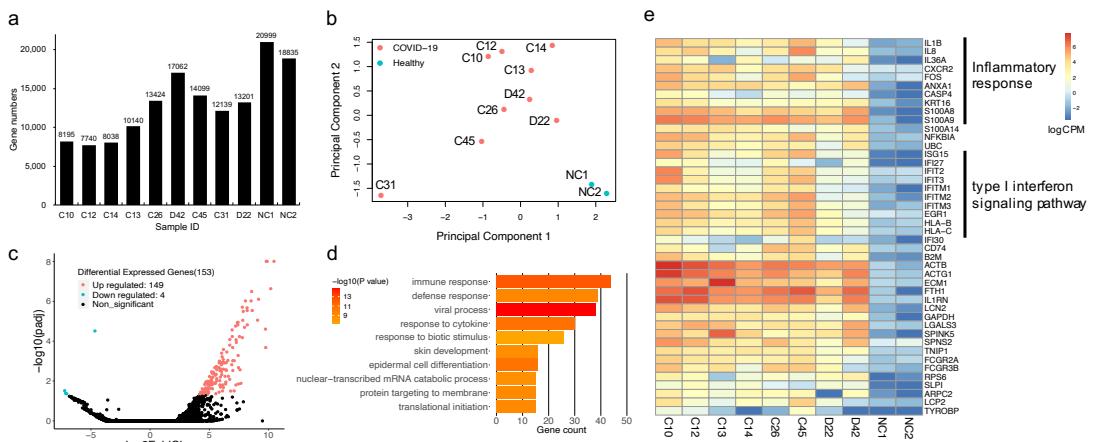
520



521

522 **Figure 3.** Microbiome profiles in COVID-19 patients and healthy individuals. **a.**
523 Histogram showing percentage of reads mapping to human, viruses, bacteria
524 and fungi for the individual samples. **b.** PCoA of microbiome using relative
525 abundance at the genus level. **c.** Heatmap showing relative abundance of
526 potential respiratory pathogens identified in SARS-CoV-2 positive and negative
527 samples. RPM: reads per million non-host reads. **d.** Heatmap displaying
528 relative abundance of antibiotic resistance genes in SARS-CoV-2 positive and
529 negative samples.

530



532 **Figure 4.** Profiling of host transcriptional response. **a.** Bar plot showing gene
533 numbers detected in each sample. **b.** MDS plot showing variation among
534 samples based on host transcriptional profiles. **c.** Volcano plot showing
535 differentially expressed genes between SARS-CoV-2 positive and negative
536 samples. Significantly up- and down-regulated genes ($padj < 0.05$,
537 $|log2FoldChange| > 1$) are highlighted in red and blue, respectively. **d.** Bar plot
538 of the most enriched Gene Ontology terms. **e.** Heatmap presenting the
539 differentially expressed immune response related genes between SARS-CoV-
540 2 positive and negative samples.